Journal of Neuroscience Methods 306 (2018) 57–67

Contents lists available at ScienceDirect

Journal of Neuroscience Methods

journal homepage: www.elsevier.com/locate/jneumeth

Massively parallel *C. elegans* tracking provides multi-dimensional fingerprints for phenotypic discovery

Michele Perni[a,1], Pavan K. Challa[a,1], Julius B. Kirkegaard[b,1], Ryan Limbocker[a], Mandy Koopman[c], Maarten C. Hardenberg[c], Pietro Sormanni[a], Thomas Müller[a], Kadi L. Saar[a], Lianne W.Y. Roode[a], Johnny Habchi[a], Giulia Vecchi[a], Nilumi Fernando[a], Samuel Casford[a], Ellen A.A. Nollen[c], Michele Vendruscolo[a,*], Christopher M. Dobson[a,*], Tuomas P.J. Knowles[a,*]

[a] *Centre for Misfolding Diseases, Department of Chemistry, University of Cambridge, Cambridge, CB2 1EW, UK*
[b] *Department of Applied Mathematics and Theoretical Physics, University of Cambridge, Cambridge, CB3 0WA, UK*
[c] *University of Groningen, University Medical Center Groningen, European Research Institute for the Biology of Aging, 9713 AV, Groningen, The Netherlands*

HIGHLIGHTS

- The Wide Field-of-View Nematode Tracking Platform can monitor for more than 5.000 animals in parallel.
- The platform extracts features important for characterising the behaviour of *C. elegans*, a widely used model organism in biomedical research.
- The platform provides a high power of detection for small changes in behaviour and reduces the risk of false positive results.
- The platform capabilities are illustrated by screening potential drugs for neurodegenerative disorders such as Parkinson's and Alzheimer's disease.
- Full details for assembling the platform, and the provision of open source codes makes it readily accessible to the community.

ARTICLE INFO

Article history:
Received 4 September 2017
Received in revised form 27 January 2018
Accepted 11 February 2018
Available online 13 February 2018

Keywords:
Neuroscience
Automation
Drug discovery
Alzheimer's Disease
Parkinson's Disease

ABSTRACT

Background: The nematode worm *C. elegans* is a model organism widely used for studies of genetics and of human disease. The health and fitness of the worms can be quantified in different ways, such as by measuring their bending frequency, speed or lifespan. Manual assays, however, are time consuming and limited in their scope providing a strong motivation for automation.
New method: We describe the development and application of an advanced machine vision system for characterising the behaviour of *C. elegans*, the Wide Field-of-View Nematode Tracking Platform (WF-NTP), which enables massively parallel data acquisition and automated multi-parameter behavioural profiling of thousands of worms simultaneously.
Results: We screened more than a million worms from several established models of neurodegenerative disorders and characterised the effects of potential therapeutic molecules for Alzheimer's and Parkinson's diseases. By using very large numbers of animals we show that the sensitivity and reproducibility of behavioural assays is very greatly increased. The results reveal the ability of this platform to detect even subtle phenotypes.
Comparison with existing methods: The WF-NTP method has substantially greater capacity compared to current automated platforms that typically either focus on characterising single worms at high resolution or tracking the properties of populations of less than 50 animals.
Conclusions: The WF-NTP extends significantly the power of existing automated platforms by combining enhanced optical imaging techniques with an advanced software platform. We anticipate that this approach will further extend the scope and utility of *C. elegans* as a model organism.

1. Introduction

Characterized by a simple anatomy, short lifespan, and well-established genetics, the nematode worm *Caenorhabditis elegans* has become a powerful modelorganism in biomedical research, in particular for genetic studies (Dillin et al., 2002; Hamilton et al.,

* Corresponding authors.
E-mail addresses: mv245@cam.ac.uk (M. Vendruscolo), cmd44@cam.ac.uk (C.M. Dobson), tpjk2@cam.ac.uk (T.P.J. Knowles).
[1] Those authors made equal contributions to this study.

https://doi.org/10.1016/j.jneumeth.2018.02.005
0165-0270/

2005; Jorgensen and Mango, 2002; Kim and Sun, 2007; Lee et al., 2003; Morley et al., 2002; Nollen et al., 2004; Sarin et al., 2008; Van der Goot et al., 2012; Van Ham et al., 2010, 2008) and drug screening (Alavez et al., 2012; Habchi et al., 2016, 2017; Perni et al., 2017a; Wu et al., 2006). The worms are small (ca. 1 mm in length), transparent, easy to manipulate, with a short maturation period of 3 days from egg to adult at 25 °C, and a life-span between 2 and 3 weeks, characteristics which facilitate the rapid study of multiple aspects of their biology (Brenner, 1974). Nevertheless, they have a cellular complexity and tissue-specific protein expression profile comparable to that of higher organisms. As a result, *C. elegans* is commonly employed as a model organism for the characterization of the molecular mechanisms underlying neurodegeneration, in particular protein aggregation (Habchi et al., 2016; Link, 1995; Morley et al., 2002; Nollen et al., 2004; Perni et al., 2017a; Van Ham et al., 2008). In this context, it has been widely employed as a molecular tool for the identification of age-related genes and pathways (Dillin et al., 2002; Hamilton et al., 2005; Jorgensen and Mango, 2002; Kim and Sun, 2007; Lee et al., 2003; Morley et al., 2002; Nollen et al., 2004; Sarin et al., 2008; Van der Goot et al., 2012; Van Ham et al., 2008, 2010) and also for the definition and characterization of promoters and inhibitors of protein aggregation (Gidalevitz et al., 2009; Morley et al., 2002; Van Ham et al., 2010), as well for monitoring the effects of small molecules (Alavez et al., 2012; Van der Goot et al., 2012; Habchi et al., 2016, 2017; Perni et al., 2017a) on such processes.

The health and fitness of *C. elegans* has conventionally been quantified in liquid media by counting the number of body bends per minute (BPM) (Gidalevitz et al., 2009; Morley et al., 2002; Van Ham et al., 2010), or by measuring the speed of movement of the worms (Machino et al., 2014; Nussbaum-Krammer et al., 2015; Swierczek et al., 2011). Other key readouts in such studies are lifespan and paralysis which have, for example, recently led to major discoveries in the field of ageing, including the identification of specific genes (Hsin and Kenyon, 1999; Kenyon, 2010; Klass, 1983) and compounds (Alavez et al., 2012) modulating longevity, the link between oxidative stress and mitochondrial function (Dillin et al., 2002; Hamilton et al., 2005; Jorgensen and Mango, 2002; Kim and Sun, 2007; Lee et al., 2003; Sarin et al., 2008), and the triggers for neurodegenerative disease (Chiti and Dobson, 2006, 2017; Knowles et al., 2014; Soto, 2003). Although manual measurements of body bends and speed of swimming movement have yielded many important insights (Alavez et al., 2012; Gidalevitz et al., 2009; Morley et al., 2002; Nollen et al., 2004; Nussbaum-Krammer et al., 2015; Van der Goot and Nollen, 2013), such studies are often hindered by difficulties in acquiring high quality data with sufficient statistical power to enable subtle behavioural patterns to be identified and measured, not least as a result of limitations in the numbers of animals that can be efficiently investigated. Manual assays remain low throughput, highly labour intensive and time consuming, and are prone to errors and to intrinsic human biases. Therefore, there are strong motivations to replace manual counting with reproducible, bias-free, time and cost effective automated measurements.

Several laboratories have recently developed innovative solutions that allow high-sensitivity measurements and accurate tracking for both single (Faumont et al., 2011; Leifer et al., 2011; Stirman et al., 2011; Tsibidis and Tavernarakis, 2007; Wang and Wang, 2013; Yemini et al., 2013) and multiple (Ramot et al., 2008; Restif et al., 2014; Swierczek et al., 2011) worms. The most recent developments have greatly improved reproducibility and sensitivity in studies of *C. elegans* relative to conventional manual procedures (Husson et al., 2012). There are, however, further exciting opportunities for enhancing the level of automation of behavioural screening of *C. elegans*. Such opportunities include the development of new approaches for the simultaneous analysis of the behavioural parameters of an entire population of worms, and connecting in a robust way paralysis and behavioural assays. In this context, a number of technical difficulties need to be overcome, such as the background clutter of existing worm tracks and eggs on the culture medium, and the identification of interactions or crossover events between animals. It is also important to be able to track a large number of worms that bend at high speed (up to 2 bends/second for young animals). Moreover, as a result of the high intrinsic variability of worm behaviour (Lublin and Link, 2013), drug treatment studies often lead to subtle phenotypic changes, and require a large number of animals to be screened in order to acquire robust datasets. Furthermore, recent studies have shown that a high power of detection (POD) is necessary to detect with confidence any significant change in behaviour and to limit false positive results (Petrascheck and Miller, 2017).

Our approach to overcoming such technical challenges has involved the development of a wide field-of-view nematode-tracking platform (WF-NTP), which enables the simultaneous investigation of multiple phenotypic readouts on large worm populations. The WF-NTP was initially developed for drug screening purposes, although it has proved to have much more general applications including the characterisation of mutant strains and very detailed behavioural studies. The WF-NTP monitors up 5000 animals in parallel, and the phenotypical readout includes multiple parameters. We used modular optical and mechanical components, giving the tracker the potential to be readily customized in the future for even more complex behavioural studies, such as the analysis of chemotaxis and learning, and for genetic studies, including high-throughput RNAi screens. During its development stage, this platform has already brought significant advantages to AD (Aprile et al., 2017; Habchi et al., 2016, 2017) and PD (Perni et al., 2017a,b) drug discovery programmes, helping the assessment of candidate compounds and the development of effective protocols for drug screening.

2. Materials and methods

2.1. Machine vision hardware

A GS3-U3-60QS6 M 1" Grasshopper USB 3.0 monochrome camera (Point Grey, Richmond, CA; 14 bits; 2736 × 2192 pixels) was combined with a 16 mm focal length high resolution lens f/1.8 – f/16 to image a 6–14 cm plate or a multi-well device under bright-field illumination (8" × 8" white AI side-fired backlight) (Edmund Optics Ltd.). All tracking was performed on a custom assembled computer with an Intel® Core™ i7-5960X @ 3.00 GHz processor and 64 GB of RAM. Images were recorded using the FlyCapture Software Development Kit (SDK) USB 3.0 (Point Grey Research Inc, Richmond, Canada).

2.2. Image analysis

Custom software written in Python (Python Software Foundation, Wilmington, Delaware, USA) was used to generate a Graphical user interface (GUI) to set up image processing and experimental parameters, such that once tracking is completed the software captures frames stored with the camera in the.avi format. Our software is called WF-NTP and is available under an open-source license (GPL); the version used in this study is available as Supplementary Software 1. Python is required to run and to modify the WF-NTP code. Our code initially detects and subtracts the background signal, consisting of non-moving objects such as small particles and shadows from the agar plate, and offers an alternative approach to removing the background without using temporal information. The method begins by defining a Gaussian adaptive threshold of the

image. Through this process essentially all worms are identified, but with a high level of false-positive pixels. Afterwards, all pixels marked as worms are then recalculated by interpolating from pixels not marked as worms. After this operation, the remaining labelled regions are identified as individual worms and the positions of these regions are then stored for each frame. The eccentricity of each tracked worm, a measure of the ratio of the major and minor ellipse axes, can then be used to estimate the extent of worm bending as a function of time. The software also outputs in parallel with the analysis a thresholded video, which allows the user to readily check for the robustness of single worm tracking and of the parameters used for the tracking. Metrics generated through this strategy include body bends, speeds, paralysis rates, area per animal, and mean errors. The fingerprint tool creates a radar chart of selected strains and parameters when loading the text files, which are created during the analysis, into the fingerprint software.

2.3. C. elegans cultures

Standard conditions were used for the propagation of *C. elegans* (Brenner, 1974). Briefly, the animals were synchronized by hypochlorite bleaching, hatched overnight in M9 buffer (3 g/l KH_2PO_4, 6 g/l Na_2HPO_4, 5 g/l NaCl, 1 μM $MgSO_4$), and subsequently cultured at 20 °C on nematode growth medium (NGM) ($CaCl_2$ 1 mM, $MgSO_4$ 1 mM, cholesterol 5 μg/mL, 250 μM KH_2PO_4 pH 6, Agar 17 g/L, NaCl 3 g/l, casein 7.5 g/l) plates seeded with the *E. coli* strain OP50. Saturated cultures of OP50 were grown by inoculating 50 ml of LB medium (tryptone 10 g/l, NaCl 10 g/l, yeast extract 5 g/l) with OP50 and incubating the culture for 16 h at 37 °C. NGM plates were seeded with bacteria by adding 350 μl of saturated OP50 to each plate and leaving the plates at 20 °C for 2–3 days. On day 3 after synchronisation, the animals were placed on NGM plates containing 5-fluoro-2′deoxy-uridine (FUDR) (75 μM, unless stated otherwise) to inhibit the growth of offspring.

For multi-well studies, worms were transferred from seeded NGM plates at the L4 stage to the multi-well plates. Worms were suspended in a solution of S Medium at 75 worms/mL containing 5 mg/mL OP50, FUDR (final concentration 120 μM) that was introduced to each well from a concentrated 0.6 mM solution to prevent the development of future generations. The compounds whose effects on the worms were to be investigated were added in appropriate quantities of water (in the case of thioflavin-T) or 0.6% DMSO (in the case of curcumin and bexarotene) at the late L4 stage such that the concentration of OP50 became 4 mg/mL. Videos for the determination of motility were then recorded at day 5 of adulthood. This protocol was adapted from previous studies (Habchi et al., 2017; Solis and Petrascheck, 2011) and optimised for the analysis of motility.

2.4. Strains of C. elegans

The following strains of *C. elegans* were used: zgIs15 [P(unc-54): αsyn:YFP]IV (OW40), where α-synuclein fused to YFP relocates to inclusions, which are visible as early as day 2 after hatching and that increase in number and size during ageing of the animals up to late adulthood (Day 17) (Van Ham et al., 2008); rmIs126 [P(unc-54)Q0:YFP]V (OW450), in which YFP alone is expressed and remains diffusely localized throughout ageing (Van Ham et al., 2008); dvIs14 [(pCL12) *unc-54*:beta 1–42 + (pCL26) *mtl-2*:GFP] (Cl2120), where *mtl-2*:GFP produces strong constitutive intestinal expression of GFP at all developmental stages and also expresses the 42 residues of the human amyloid-β peptide. In this strain, accumulation of $A\beta_{42}$ aggregates and their associated toxicity is enhanced at temperatures higher than 20 C° (Fay et al., 1998); dvIs50 [pCL45 (*snb-1*:Abeta 1–42:3′ UTR(long) + *mtl-2*:GFP]I, which shows pan-neuronal expression of the human $A\beta_{42}$ peptide and constitutive intestinal expression of GFP from a marker transgene; the strain shows deficits in chemotaxis, associative learning, and body bends in liquid, and incomplete sterility due to germline proliferation defects and embryonic lethality (Wu et al., 2006); dvIs100 [unc-54p:A-beta-1-42:unc-54 3′-UTR + mtl-2p:GFP] (GMC101), which produces constitutive expression of GFP in intestinal cells; unc-54p:A-beta-1-42 which expresses in the body-wall muscle cells the full length human $A\beta_{42}$ peptide that aggregates in vivo; shifting L4 or young adult animals from 20 °C to 25 °C causes paralysis (McColl et al., 2012). dvIs15 [(pPD30.38) unc-54(vector) + (pCL26) mtl-2:GFP] (Cl2122) was used as a control strain for CL2120, GMC101 and CL2355, and shows an apparently wild type phenotype (Fay et al., 1998; McColl et al., 2012; Wu et al., 2006).

2.5. Manual motility assay

Animals of different ages were placed in a drop of M9 buffer and allowed to recover for 30 s (to avoid the observation of behaviour associated with stress) after which the number of body bends was counted for either 30 s or 1 min. For blinded motility assays, adult animals were randomly picked from the treated and untreated populations and measured for motility without knowledge of the concentration of the added compound. 50 animals were counted in each experiment unless stated otherwise; the experiments were carried out in triplicate and the data from one representative experiment are shown in each figure. Statistical analysis was performed using Graphpad Prism software (GraphPad Software, San Diego, CA, USA) (Gidalevitz et al., 2009).

2.6. Automated motility assay on agar plates

All *C. elegans* populations were cultured at 20 °C and developmentally synchronized from a 4 h egg-lay. At 64–72 h post egg-lay (time zero) individuals were transferred to FUDR plates, and body movements were assessed over the times indicated. At different ages, the animals were washed off the plates with M9 buffer and spread over an OP-50 unseeded 9 cm plate, after which their movements were recorded at 20 fps using the WF-NTP for 30 s or 1 min. Up to 1000 animals were counted in each experiment unless stated otherwise, and one experiment that is representative of the three types of measurement is shown. Videos were analysed using a custom made tracking code which records different metrics, including body bends/min, swimming speed, and paralysis assays; we considered that worms showing less than 5 body bends/min and moving at less than 1 mm/min to be paralysed. The software is provided as open-source and can be downloaded online as Supplementary Software 1.

2.7. Automated motility assay on multi-well plates

For screening the multiwell plates, worms were stored at 20 °C prior to the L4 stage and at 20 °C or 23.5 °C thereafter for OW40 or GMC101 worms, respectively; these temperatures were found sufficient to induce a phenotype. Prior to screening, a bench top plate shaker was used at 750 rpm for 1 min to distribute sedimented OP50 and induce full worm motility. Immediately after shaking, the worms were staged on the platform and the file collection was initiated 60 s after shaking for 1 min at 20 fps. 24 wells were analysed per condition corresponding to approximately 250 worms.

2.8. Analysis of collision rates and recording times

All *C. elegans* populations were cultured at 20 °C and developmentally synchronized from a 4 h egg-lay. At 64–72 h post egg-lay (time zero) ca. 5000 wild type worms were transferred to FUDR

plates and allowed to develop until D4 of adulthood. The D4 adults were washed off the FUDR with M9 buffer and concentrated via centrifugation. The supernatant was then removed and the worms were then resuspended in 3 ml M9 before being counted to determine their concentration. The worms were then transferred onto 9 cm OP50 unseeded NGM plates, after which their movements were recorded at 20 fps for 1 min and their number was analysed using the WF-NTP. The parameter "memory" was also set at 0 or 40 frames, to determine the collision rate modification in its presence of absence, respectively. For measurement of the body bends/min over time, worm movements were recorded at 20 fps using the WF-NTP platform for 30 s, 60 s, 120 s and 180 as, after which their motility was analysed. Up to 1000 worm per condition were screened.

2.9. Paralysis rates in response to paralysing agents

Adult worms were washed off the FUDR plates at day 4 of adulthood using 15 ml of M9 buffer and were subsequently concentrated to 4 worms/μL; the worms were then transferred to 1.5 ml microcentrifuge tubes with 400 worms per sample. Paralysing agents were added to the worms at 0, 0.1, 0.5, 1, 5, 10 and 50 μM for sodium azide and 0, 1, 5, 10, 50, 100 and 500 μM for levamisol (total volume 1 ml) and incubated at room temperature for 10 mins on an orbital shaker at 755 RPM to prevent sedimentation. After incubation samples were washed with M9 buffer and screened at 20 fps using the WF-NTP for 1 min. Videos were then analysed and we considered worms showing less than 5 body bends/min and moving at less than 1 mm/min to be paralysed.

2.10. Biological and technical replicas

To assess technical reproducibility, all *C. elegans* populations were cultured at 20 °C and developmentally synchronized from a 4 h egg-lay. At 64–72 h post egg-lay (time zero) 5000 worms were transferred to 5 FUDR plates, and body movements were assessed at day 4 of adulthood. Here, animals on each plate were washed off using M9 buffer and spread over an unseeded 9 cm NGM plate in 5 ml M9 buffer, after which their movements were recorded at 20 fps using the WF-NTP for 1 min. Up to 1000 animals were counted in each experiment unless stated otherwise. Videos were analysed using a custom tracking code which evaluates different metrics, including frequency of body bends, swimming speed, and paralysis assays; we considered that worms showing less than 5 body bends/min and moving at less than 1 mm/min to be paralysed.

The same process was followed for assessing biological reproducibility, however, for these experiments only 1000 worms from separate synchronisation procedure were taken and screened on day 4 of adulthood. This was repeated for 4 separate synchronisation steps, each originating from a different batch of worms.

3. Results

3.1. Development of the wide field-of-view tracking platform

In order to overcome the technical challenges in automated tracking, we developed a platform that allows data acquisition on a full Petri dish or multi-well plate while still maintaining a resolution appropriate for the simultaneous tracking of multiple nematodes and for defining multiple phenotypes for each animal. This approach has the advantage of offering much higher rates of throughput, while at the same time facilitating the screening of dilute suspensions of worms over a larger surface area, reducing significantly the chance of overlap and collisions.

To image a given object, the choice of the light source, the optical components and the detector are strongly interrelated. We used an array of LEDs coupled to a diffuser to produce uniform illumination over an area of 20 cm by 20 cm with minimal heat production. The uniformity of light diffusion, compared to conventional lamps, improves the contrast of the image, avoids blooming and shadowing, and the low heat illumination avoids stressing the worms and affecting their behaviour during observation. The imaging was achieved with a combination of 8 lens components (Fig. 1), which allow operation with dishes of different sizes (such as 6, 9 cm and 14 cm) and multi-well plates. The imaging objective minimizes errors of parallax and perspective and ensures adaptable magnification, field-of-view and focal length. Finally, a camera with high resolution, high sensitivity and rapid imaging rate was used as the detector (see Materials and Methods for technical details). Through this strategy, we achieved data acquisition over surfaces as large as 20 cm in diameter, while maintaining high resolution and high imaging rates.

The imaging platform designed in this work also allows simultaneous detection of nematodes both swimming in liquid and when crawling in a thin layer of bacteria on an agar surface. Data for swimming worms were acquired continuously at a time resolution of 20–30 frames per second (fps), and 3–7 fps for studies focused on crawling. Data for movement on a surface were typically obtained by imaging an area of over 250 cm^2, with a lateral resolution down to 35 μm, allowing the imaging of 6, 9 or 14 cm agar plates or a multi-well plate (Figs. 1a, 2b). To image different fields of view depending on the choice of plate, the distance between the sample and the imaging lens can also easily be varied (Fig. 1a and Fig. 1, S1). Moreover, the modular structure of the tracking platform makes it easily accessible, reproducible and highly customizable (Fig. 1, S1).

3.2. Worm tracking software platform

The software packages that are generally employed for visual analysis of nematodes use static background subtraction, which works well but can have limitations in cases where not all the worms are alive and moving significantly in the time-frame of the recording (Husson et al., 2012). Indeed, if any worms are paralysed or dead, this approach can skew the final statistics, as background subtraction can include images of immobile animals. Moreover, the inclusion of paralysis and death rates in the analysis of worm populations is particularly important in the case of screens for potential therapeutic leads, as molecules designed to improve worm fitness are also likely to influence survival and paralysis rates (Ramot et al., 2008).

We have therefore developed a software package available on an open source basis and completely customizable (Software 1). It detects and subtracts background images (i.e. of objects other than those of the worms) from the set of video images, by means of an adaptive threshold filter (Fig. S1). The procedure first defines a Gaussian adaptive threshold of the image, and then recalculates all the pixels identified to show nematodes by interpolating from those pixels that do not show images of worms. We chose this approach to avoid removing the immobile worms as part of the background signal, and it offers a strategy for the removal of background noise without using temporal information. In this way, paralysed worms can be analysed in parallel with moving ones and included in the final statistics (see Materials and Methods for details). The software also provides access to a simple process of removing all the non-moving particles through a more conventional approach. While it is critical in studies associated with drug discovery to include paralysed animals to achieve a robust analysis, this alternative methodology can be employed as internal, complementary validation of the results, or in studies where the behaviour of the fraction of worms that are moving is of primary interest. These methods of subtracting background effects are iden-

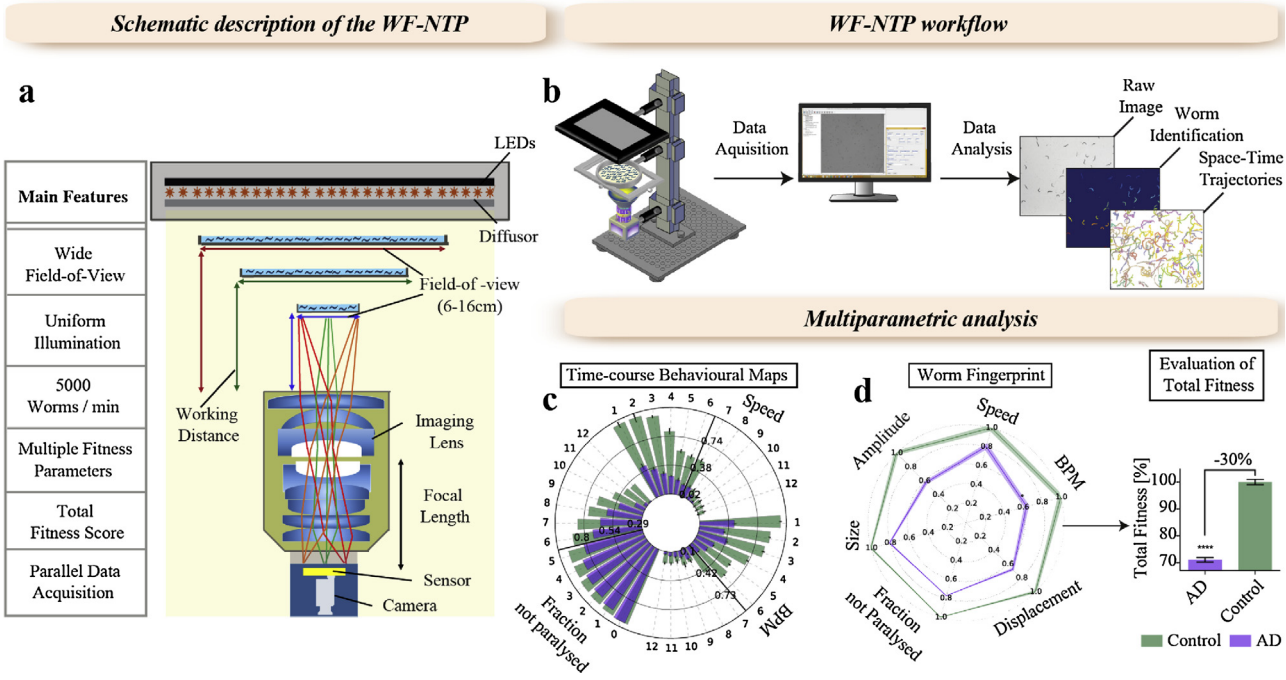

Fig 1. Overview of Wide Field-of-view Nematode Tracking Platform (WF-NTP). (a) Details of the tracker geometry: worms crawling or swimming on agar plates are imaged from below using a machine vision camera mounted on an imaging lens. Multiple trackers can be easily assembled and used to image 6, 9 and 14 cm agar plates or multi-wells plates. (b) Examples of the main tracking steps are shown (see Materials and Methods for details). (c) The behavioural map characterises a worm model of Alzheimer's disease (AD) (McColl et al., 2012) (violet) and related controls (green) maintained for 12 days at 24 °C, and shows the variations of the speed of movement, bend frequency and paralysis rate, related to day 0 wild type worms. In this model the temperature increase leads to age-dependent progressive muscle paralysis. The outer numbers indicate the days of adulthood of the study. (d) An example of fingerprinting of worm phenotypes and generation of the related "total fitness" score; metrics of the control CL2122 worms (McColl et al., 2012) are shown in green, and GMC worms (McColl et al., 2012), which express $A\beta_{42}$ in the muscle cells (AD), are shown in violet. In comparison to healthy controls, overexpression of $A\beta_{42}$ in muscle cells causes a significant decrease in speed, body bends/min (BPM), bend amplitude, and bend displacement (which measures how far a worm propels itself with a single body bend), together with a decrease in the moving fraction (the paralysis rate) and the size of the worms. These parameters can be readily monitored in parallel by using the WF-NTP. The fingerprint and the total fitness score were produced for animals at day 5 of adulthood. (For interpretation of the references to colour in this figure legend, the reader is referred to the web version of this article.)

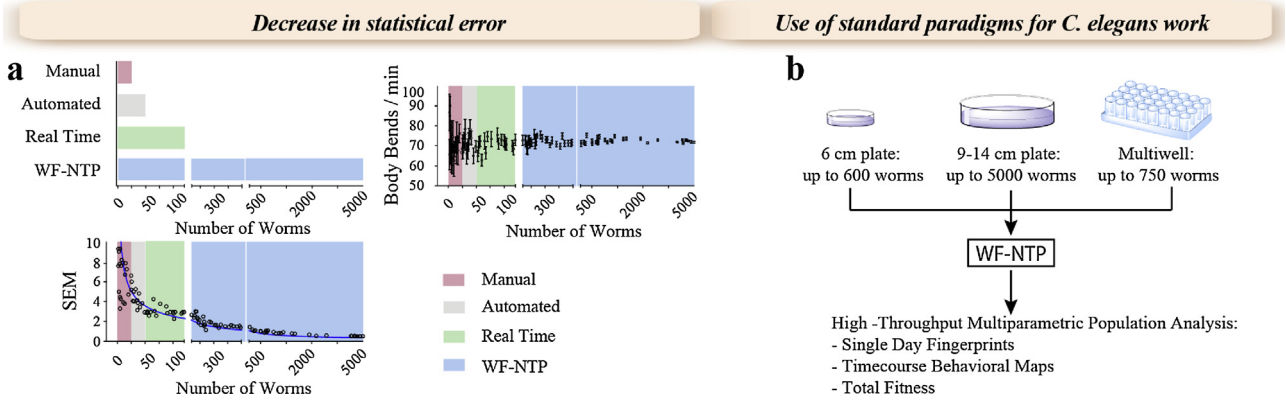

Fig. 2. WF-NTP performance and applications. (a) The left panel shows the maximum number of animals tracked with the WF-NTP (blue bar), manual (pink bar) and other automated platforms (grey bar) and real time (green bar) platforms. The right and bottom panels show the correlation between the standard error of the mean (SEM) (related to the BPM) and the number of animals analysed. The WF-NTP platform (blue) facilitates the tracking of over 5000 worms thereby markedly reducing the SEM (middle and right panels) by ca. 14-fold related to a standard sample for manual screening of ca. 25 worms (red) and ca. 6-fold related to other automated platforms (grey). The plots are representative of the motility (BPM) of wild type (N2) worms (Brenner, 1974) at day 6 of adulthood and the errors bars represent the SEM. The red area represents the number of animals counted on average for manual screenings (<25); the grey area indicates the maximum throughput achievable with previously described automated trackers, off-line (<50) and in real time (<120) (Swierczek et al., 2011); the light blue areas represent the number of animals that can be analysed with the WF-NTP (<5000). For every measurement, the animals were randomly selected between the screened worm populations. Data were fitted to $1\sqrt{(n)}$ (blue line in the bottom panel) for the SEM. (**b**) The WF-NTP can be used in combination with standard procedures for worm studies, such as 6, 9 and 14 cm agar plates, and multi-well plates for liquid cultures. (For interpretation of the references to colour in this figure legend, the reader is referred to the web version of this article.)

tified here as 'z-filtering' and 'keep dead' methods, and they can also be run in parallel.

A GUI (Fig. 1, S1) was also developed to facilitate the analysis of the defined locations of regions of interest (ROIs) and to identify quickly and easily behavioural changes in high-throughput screens, particularly in multi-well plates. In addition, a subset of utilities was also generated to visualize and interpret the data (see Materials and Methods for details), such as a "plot path" tool, which makes it possible to plot the movements of the individual nematodes, and to facilitate the visual analysis of their motion. In order to

reduce further the problem posed by worm overlap and crossover, the code provides a computational solution for worms that overlap for a few frames; this issue can be regulated by means of the parameter labelled as "memory", and accessible in the GUI. As a further internal quality control check for the tracking of individual animals, the code outputs a video that shows the behaviour of individual worms. Moreover, it is possible to output an example of thresholding prior to initiating the analysis (Fig. 1, S2), in order to ensure that the algorithm is set up in an optimal manner. Finally, our analysis acts to avoid the underestimation of errors resulting from worms that appear to be "new" worms because of collisions and overlap; the software also provides an upper limit on the errors by considering the maximum number of worms detected in a single frame, rather than the total number of worms detected in the entire video (see Material and Methods for details).

3.3. Analysis of statistical power

Many of the current worm-tracking platforms focus on the observation of the behaviour of single worms by imaging at high resolution (Faumont et al., 2011; Hardaker et al., 2001; Husson et al., 2012; Leifer et al., 2011; Stirman et al., 2011; Tsibidis and Tavernarakis, 2007; Wang and Wang, 2013; Yemini et al., 2013). Others are designed to enable automated simultaneous tracking of up to about 50 animals at a lower resolution (Chalasani et al., 2007; Husson et al., 2012; Ramot et al., 2008). The use of a real-time strategy has enabled up to 100 worms to tracked in parallel (Swierczek et al., 2011), and this approach has also addressed the issue posed by acquiring and storing long high-resolution videos, which involves very large files, by eliminating the need for such storage. In the present work, our aim has been to develop a platform to provide both massively parallel tracking capabilities and the possibility of storing the data for subsequent analysis, while still maintaining the high resolution and sensitivity that is required for statistically significant analyses (Petrascheck and Miller, 2017). The WF-NTP platform described here can readily track up to 5000 animals in parallel (Figs. 1–2), thereby increasing throughput by about three orders of magnitude relative to manual approaches and by about 50 times compared to existing trackers (Husson et al., 2012): (Fig. 2). As the standard error of the mean (SEM) of a given measurement is proportional to the inverse of the square root of the sample size, an increase in the number of individuals that can be tracked therefore results in a significant reduction of statistical errors.

3.4. Multi-parametric analysis

The application of this novel tracking procedure allows the extraction and analysis of parallel multi-parametric features describing the behaviour of a population of nematodes, such as their bending frequency, size, speed and paralysis rates (Gidalevitz et al., 2009; Morley et al., 2002; Van Ham et al., 2010) together with recently defined behavioural parameters such as bending amplitude (Nahabedian et al., 2012), which can be used to reveal new aspects of disease-associated phenotypes. The multi-parametric analysis enables evaluation of the complex phenotypes of the worms; indeed it has recently been described how multi-parametric analysis can reveal undiscovered correlations between different aspects of worm behaviour, for example between the velocity of the animals and their lifespan (Hahm et al., 2015). To this end, we have included in the GUI the option to characterize quantitatively the unique behavioural patterns of *C. elegans*, by the means of fingerprints and behavioural maps (Fig. 1b–d), which can be generated easily to provide a visual representation of multiple quantified metrics describing the behaviour of the animals, such as body bend frequency, paralysis rate, bend amplitude, displacement per bend, speed of movement and size. Furthermore, this multi-parametric analysis allows the combination of the different metrics into a single value, which we call the total fitness, representing the overall vitality of a very large population of worms (Fig. 1d). Indeed, recent studies highlight the key importance of multi-parametric behavioural profiling for achieving an accurate and sensitive characterization of mutant strains (Faumont et al., 2011; Leifer et al., 2011; Stirman et al., 2011; Tsibidis and Tavernarakis, 2007; Wang and Wang, 2013; Yemini et al., 2013), as well as illustrating the importance of multi-parametric analysis. Finally, we anticipate that further development of the open source software will extend significantly the number of phenotypes that can be distinguished, hence making *C. elegans* fingerprinting yet more sensitive and representative of the complex behaviour shown by *C. elegans*.

3.5. Application of WF-NTP to the study of models of neurodegenerative diseases

We show in Fig. 2 the dramatic reduction in the standard error of the mean that results from an increase in the population size that is enabled by the use of the WF-NTP platform. In order to explore the biological relevance of this reduction in error we have applied the WF-NTP to the characterization of a number of well established behavioural metrics, including paralysis rate, bend frequency and speed of movement, to several well-established worm models of neurodegenerative disorders (Figs. 3–5); these models include one related to Parkinson's disease (PD) (Van Ham et al., 2008), and three to Alzheimer's disease (AD) (Fay et al., 1998; McColl et al., 2012; Wu et al., 2006), in which the worms were grown at different temperatures in order to induce changes in motility. In the PD model, α-synuclein is overexpressed in the body-wall muscle cells, the same location in which $A\beta_{42}$ is over-expressed in two AD models (Aβ $Muscular_{I,II}$). The expression of these aggregation-prone proteins in body wall muscles, as well as in neurons (Lublin and Link, 2013), has been shown to result in a decrease in motility with age relative to control worms. The differences in phenotypes between worm models of neurodegenerative disorders can however be quite subtle and difficult to detect due to the intrinsic high variablity that exists within a given worm population.

To address this issue, the use of the WF-NTP has enabled us to collect in parallel data that relate to several different behavioural metrics, including bending, swimming speed and paralysis rate (Figs. 3–4) for the PD (Van Ham et al., 2008) and the three AD (Fay et al., 1998; McColl et al., 2012; Wu et al., 2006) disease models and their controls; in all four disease models phenotypical changes were evident in the three behavioural parameters studied (Figs. 3–4). In particular, we were able to observe clear behavioural differences between a third AD strain in which $A\beta_{42}$ is over-expressed in the nervous system (Machino et al., 2014; Wu et al., 2006) (Aβ Neuronal) and the control animals (Fig. 3). These results are particularly significant as the phenotype induced by $A\beta_{42}$ expression, and in general by pan-neuronal expression, is known to be particularly mild and very challenging to detect (Machino et al., 2014). Furthermore, in another set of experiments with temperature sensitive $A\beta_{42}$ worms (McColl et al., 2012), we were able to detect subtle differences in the motility induced by very small changes in temperature (Fig. 4). In all these studies, we were able to carry out behavioural studies and to acquire simultaneusly paralysis rate information, and then to generate a time-course multiparametric behavioural maps that relate the different metrics to each other, revealing previously unrecognised phenotypic profiles (Figs. 3–4).

3.6. Applications in molecular screening

Our initial focus was to optimize the WF-NTP platform for high-throughput studies aimed towards molecular screening in the context of drug discovery. Indeed, in a previous paper, we identified

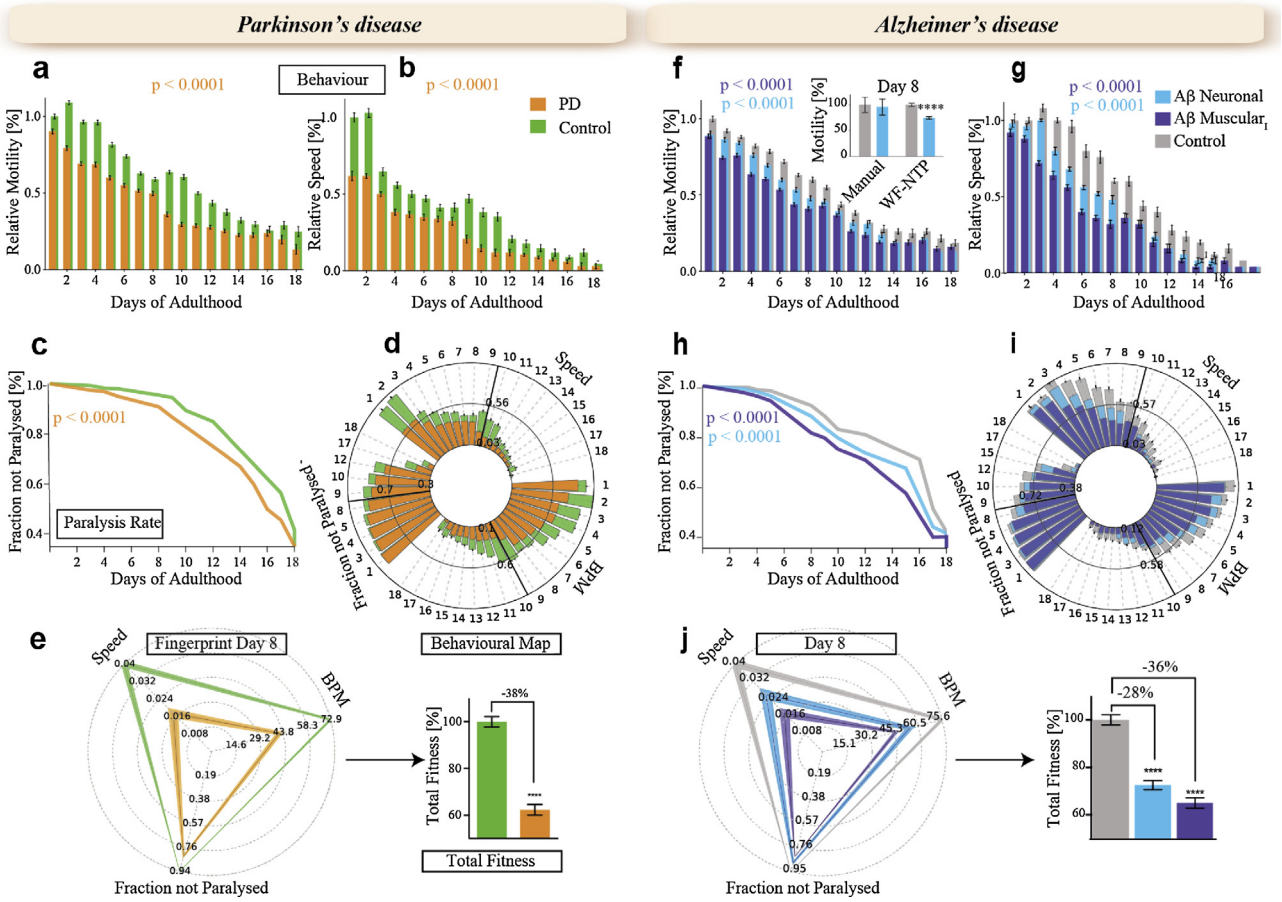

Fig. 3. Application of WF-NTP for the study of *C. elegans* models of PD and AD. (**a–c**) Motility (**a**), speed (**b**) and paralysis rate (**c**) decline with ageing for OW40 (PD) and OW450 (Van Ham et al., 2008) (control). (d) Behavioural map showing fitness decline with ageing for OW40 (Van Ham et al., 2008) (PD) compared to control OW450 worms. The fitness of OW40 (PD) worms overexpressing α-synuclein:YFP in body wall muscle cells (orange) is significantly lower than that of the OW450 (control) (green). (**e**) For each strain, a representative fingerprint plot for day 8 of adulthood, which includes readouts of body bends / min (BPM), speed and paralysis rate, is shown, together with the related total fitness score. (**f–h**) Motility (**f**), speed (**g**) and fraction not paralysed (**h**) decline with ageing for CL2120 (Fay et al., 1998) worms (Aβ muscular$_I$) and in CL2355 (Wu et al., 2006) (Aβ neuronal) and in comparison to the control CL2122. In CL2120 worms expressing the Aβ_{42} peptide an age-dependent paralysis was observed. In CL2355 worms, the expression of the Aβ_{42} peptide into the neuronal system induces an age dependent paralysis. The trackers show a significant difference between the motilities of CL2120 and CL2355 worms when compared to CL2122 controls (two-way ANOVA, $p \leq 0.0001$). The insert shows the behavioural differences in worms pan-expressing Aβ_{42} in the nervous system (Machino et al., 2014; Wu et al., 2006) (Aβ neuronal) (N = 1000) versus the control animals and comparison with manual counting (N = 25). The data were obtained at day 8 of adulthood. (**i**) Behavioural map showing fitness decline with ageing for CL2120 (Fay et al., 1998) and CL2355 (Wu et al., 2006) worms; the fitness of CL2120 worms (violet) is significantly higher than that of the Cl2122 controls (grey). Cl2355 worms (light blue) show a milder phenotype when compared to Cl2122 controls. (**j**) For each strain, a representative fingerprint plot is shown for day 8 of adulthood, which includes readouts of body bends / min (BPM), speed, and paralysis rate, and the related total fitness score. The quadruple asterisks (****) indicate, $p \leq 0.0001$ (Student's *t*-test). A two-way ANOVA was carried out for statistical significance for timecourses (****) indicate, $p \leq 0.0001$, NS = non significant. (For interpretation of the references to colour in this figure legend, the reader is referred to the web version of this article.)

a novel potential therapeutic compound for AD (Habchi et al., 2016) but we realised from this study that in order to achieve the throughput needed to screen a large number of molecules with sufficient statistical significance (Fig. 5) it would be necessary to improve substantially the sampling size (N > 200) compared to that achievable by using manual assays. As a consequence of the high throughput achieved using the platform described in the present paper, the limiting factor becomes the number of worms that can be prepared by conventional synchronous worm population techniques, rather than the number whose behaviour can be analysed. Moreover, the combination of a wide field-of-view microscope and multi-well plates or Petri dishes brings the great advantage of the ability to screen simultaneously populations of worms exposed to a wide variety of conditions, rather than carrying out such experiments sequentially, ensuring a higher degree of control over temporal and environmental factors.

To assess further the performance of the platform we investigated the influence on the models of PD (Van Ham et al., 2008) and AD (Fay et al., 1998; McColl et al., 2012; Wu et al., 2006) described above of three compounds, thioflavin T (Alavez et al., 2012), curcumin (Alavez et al., 2012) and bexarotene (Habchi et al., 2016; Wood, 2016), whose effects on protein aggregation have been studied previously using both manual (Alavez et al., 2012) and automated (Habchi et al., 2016) methods. Analysis of the effects of bexarotene in vitro showed that this compound has substantial effects on the primary nucleation step in the aggregation of Aβ_{42} (Habchi et al., 2016) and in vivo studies have indicated that this compound affects both the degradation and clearance of Aβ_{42} amyloid deposits *in C. elegans* (Habchi et al., 2016) and mice (Cramer et al., 2012). In addition, both thioflavin T and curcumin have been found to extend lifespan in a variety of worm models of neurodegenerative diseases (Alavez et al., 2012). In the study reported here, worms expressing human Aβ_{42} (McColl et al., 2012) were treated at the last stage of development before adulthood (the L4 stage) with up to 100 μM concentrations of curcumin, 200 μM concentrations of thioflavin T (Fig. 5), and up to 10 μM concentrations of bexarotene (Fig. 5). Motility was determined using the protocols described above, and a well-defined dose-dependent relationship

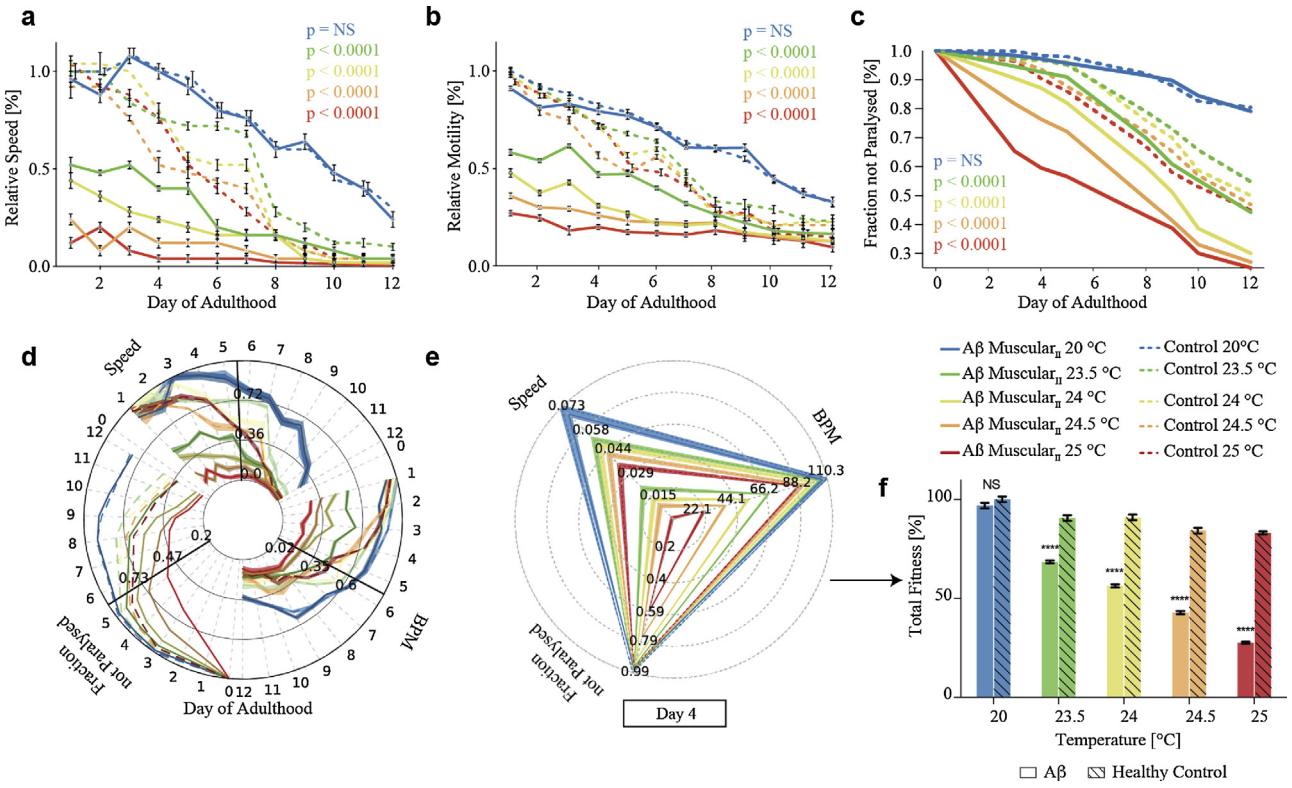

Fig. 4. The use of WF-NTP resolves subtle phenotypical differences induced by small temperature variations in $A\beta_{42}$ worms. In GMC101(Aβ/ min $Muscular_{II}$) (McColl et al., 2012) worms, the overexpression of the $A\beta_{42}$ peptide in muscle cells causes age and temperature dependent paralysis. At 20 °C the GMC101 worms do not show any differences in motility when compared to Cl2122 controls. Raising the temperature above 23.5 °C increases significantly the severity of the muscle paralysis in GMC101 worms; (a) speed, (b) body bends / min (BPM), (c) paralysis rate. (d) The behavioural map and (**e**) the worm fingerprint at day 3 of adulthood, which includes readouts of BPM, speed, and paralysis rate; (f) the corresponding total fitness score. The plot shows the behaviour at day 4 of adulthood. In all plots the solid lines represent GMC101 worms and the dashed lines represent CL2122 controls. Experiments were carried out at 20 °C (blue), 23.5 °C (green), 24 °C (yellow), 24.5 °C (orange), 25 °C (red). The single (*) asterisks indicate $p \leq 0.05$ (Student-t test), and are relative to control CL2122 worms incubated at the same temperature of the GMC101. ****, $p \leq 0.0001$ (Student's *t*-test). A two way ANOVA was carried out for statistical significance for timecourses, (****) indicate, $p \leq 0.0001$, NS = not significant. (For interpretation of the references to colour in this figure legend, the reader is referred to the web version of this article.)

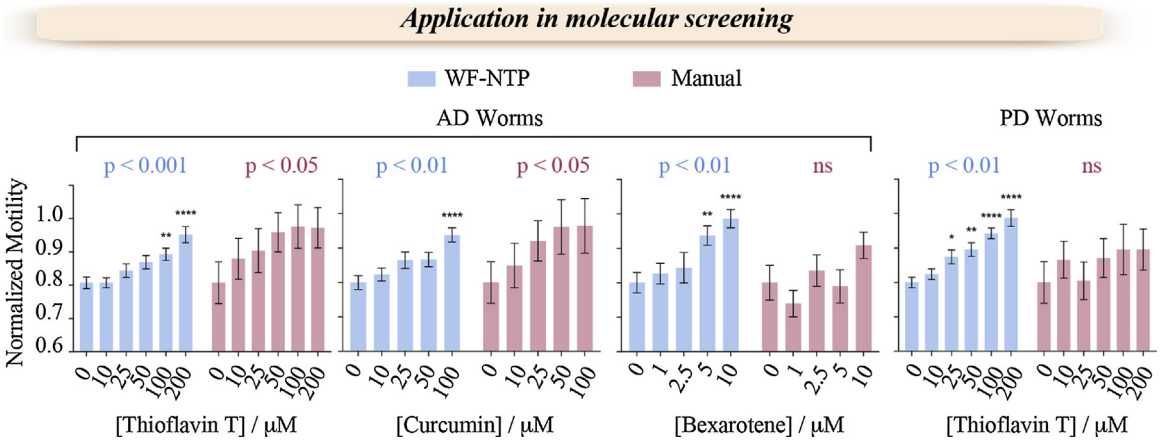

Fig. 5. Application of WT-NTP in studies of the effects of small molecules on different worm strains. Analysis of the effects of thioflavin T (0, 10, 25, 50, 100, 200 µM), curcumin (0, 10, 25, 50, 100 µM) and bexarotene (0, 1, 2.5, 5, 10 µM) on GMC worms (McColl et al., 2012) (AD) (left and centre panel), and thioflavin T treatment on OW40 (α-synuclein) worms (Van Ham et al., 2008) (PD) (right panel) using the WF-NTP (N ~ 250, blue) and compared to manual counting (N = 50, red). All plots show day 5 of adulthood, with the averaged motility normalized to the untreated group; the errors show the SEM. The single (*), double (**), and quadruple (****) asterisks indicate $p \leq 0.05$, 0.01, 0.0001, respectively, and are relative to untreated worms. The p values above each group indicate one-tailed correlation analyses of the response for WF-NTP and manual counting; ns indicates not significant. (For interpretation of the references to colour in this figure legend, the reader is referred to the web version of this article.)

between treatment and the recovery of motility was observed for all three compounds (Fig. 5). Additionally, worms expressing α-synuclein (Van Ham et al., 2008) were also treated with the same concentrations of thioflavin T, and again a strong recovery of motility was observed compared to untreated worms, with a clear dose dependence (Fig. 5).

The videos recorded for these experiments were further analysed to compare the WF-NTP procedure with conventional manual

assays, which count body bends. For each compound, and at each concentration, 50 worms were selected at random and their motilities scored. Manual counting showed that addition of thioflavin-T and curcumin increased motility, although with inconsistent dosage effects for $A\beta_{42}$ worms, but failed to identify with statistical significance that thioflavin-T influences motility in either system (Fig. 5). In all cases, by contrast, the use of the WF-NTP showed well-defined enhancements in motility with clear dose dependences, stressing the advantages of the analysis of large populations in behavioural studies of *C. elegans*.

4. Discussion and conclusions

Recent technological developments have begun to address the need for automated methods in *C. elegans* research, and a number of digital tracking platforms have been developed in the past few years to characterize worm behaviour in a significantly more detailed manner than is possible by means of manual methods (Buckingham and Sattelle, 2009; Feng et al., 2004; Hardaker et al., 2001; Husson et al., 2012; Nussbaum-Krammer et al., 2015; Stroustrup et al., 2013; Tsechpenakis et al., 2008), and hence to facilitate screening for behavioural phenotypes with greatly reduced requirements for input from the user (Chalasani et al., 2007; Leifer et al., 2011; Stroustrup et al., 2013; Swierczek et al., 2011; Yemini et al., 2013). One limitation of current automated methods for analysing the behaviour of *C. elegans* has been the number of worms that can be monitored and tracked simultaneously at high resolution, and the computational challenges posed by the overlap of animals during experiments has reduced the reliability of tracking procedures. Thus, for example, uniform illumination turns out to be an important feature, and the combination between optical and software development has been vital in this context.

A solution adopted by many laboratories has been to focus on tracking single worms at high-resolution (Faumont et al., 2011; Leifer et al., 2011; Stirman et al., 2011; Tsibidis and Tavernarakis, 2007; Wang and Wang, 2013; Yemini et al., 2013) with the aid of automated stages, which can be programmed to follow the movement of isolated animals (Faumont et al., 2011; Hardaker et al., 2001; Husson et al., 2012; Leifer et al., 2011; Stirman et al., 2011; Tsibidis and Tavernarakis, 2007; Wang and Wang, 2013; Yemini et al., 2013). This approach has allowed extreme precision in the analysis of the behaviour of individual worms, although the total throughput remains low. Despite these important developments, a very high-throughput phenotypical analysis is required for some processes, such as screening potential drugs, involving high-resolution imaging of multiple animals as well as obtaining good statistics and taking account of the extremely high heterogeneity in the behaviour of worm populations (Lublin and Link, 2013). A further challenge is the very large quantity of data associated with this type of analysis, and one solution to this problem has been to develop real-time strategies (Swierczek et al., 2011), which have been shown to allow the determination of behavioural parameters for up to 120 animals, although storing the videos for subsequent data analysis is not possible with such approaches (Husson et al., 2012).

In the present paper we have described the development and application of a tracking approach, the WF-NTP method, to monitor and to analyse multiple features of the behaviour of *C. elegans* populations in an automated manner. This approach allows simultaneous multi-parametric monitoring of up to 5000 animals, and in order to analyse their behaviour in the most efficient manner, we have combined a wide field-of-view imaging platform with the development of a machine vision software platform. This platform allows direct and simultaneous evaluation of the bending frequency, bending amplitude and displacement per bend (a direct measure of how far a worm can propel itself forward while swimming), as well as the speed of movement, body size and rate of paralysis within very large worm populations. Although the high spatial and temporal resolution of the videos necessary for this type of analysis can result in very large file sizes, our platform can work with compressed videos. The technical developments that we have incorporated in this approach include reducing the issue of overlap and crossovers of individual worms by the means of a very wide field-of-view allowing experiments to be performed with low worm densities.

The WF-NTP approach can provide parallel and multi-parametric analysis of the characteristic behaviour of *C. elegans* populations with very high sensitivity and unprecedented statistical significance. The results demonstrate the importance of wide field-of-view data acquisition to increase greatly the numbers of animals that can be monitored in a single experiment, effectively decreasing the experimental errors and greatly improving the statistical validity of the studies. Critically, our tracking procedure also has the advantage of allowing paralysis studies to be performed in parallel with other behavioural measurements, thus avoiding the final statistics becoming skewed by the presence of immobile animals. Indeed, we show that the inclusion of paralysed animals significantly improves the resolution needed for identifying potential drug candidates, even in large populations of worms (Habchi et al., 2016). These methods can be employed for the hundreds of worm strains that are currently available and that could be studied under a wide range of conditions.

We have validated the WF-NTP method by examining several models of neurodegenerative diseases and found that subtle behavioural effects, which are not readily detectable by using approaches with lower statistical power, can be reliably observed with WF-NTP, such as the identification of behavioural deficits induced by the pan-neuronal expression of the $A\beta_{42}$ peptide, or by subtle variations in temperature, or by an increase in fitness induced by the administration of small molecules such as bexarotene (Fig. 5). The technical details provided in this manuscript and the supplementary information (Fig. S1) will enable researchers readily to reproduce and adapt the platform and the modular structure of its optical components. In addition, the software that we provide as an open source code (Supplementary code 1) makes the approach readily accessible for appropriate modifications and implementation, such as the incorporation of mechanosensory or optogenetic stimuli, and hence will make the platform suitable for those studying more complex aspects of the behaviour of *C. elegans*.

In summary, we believe that the WF-NTP platform will be of great value to laboratories currently involved in studies of *C. elegans*, and will be applicable to a wide array of investigations, ranging from developmental studies to drug discovery. On the basis of the results we present in this paper, this approach should make it possible to characterize effects that are not readily detectable using conventional methods. In addition, in the light of its ease of use, low cost and convenient graphical interface, we also expect that laboratories that are not specialised in studies of *C. elegans* will readily be able to incorporate the use of this model organism in their research programmes.

Author contributions

M.P., N. F., R. L. and S.C. performed all the *C. elegans* experiments, P.K.C. designed and built the worm tracker and J.B.K. wrote the worm-tracker code and P.S., G.V., M.K. and M.C.H., implemented the associated utilities. M.P., T.M., P.K.C., J.B.K., K.L.S., M.K., R. L., E.A.A.N, M.V., C.M.D and T.P.J.K. were involved in the design of the study. M.P., P.K.C., M.V., C.M.D and T.P.J.K. wrote the paper, and all

the authors were involved in the analysis of the data and editing of the manuscript.

Competing financial interests

The authors declare no competing financial interests.

Acknowledgments

This work was supported by the Cambridge Centre For Misfolding Diseases (C.M.D., T.P.J.K. and M.V.), the Wellcome Trust (C.M.D., T.P.J.K. and M.V.), the European Research Council (ERC) (P.K.C., T.P.J.K., E.A.A.N.), the Biotechnology and Biological Sciences Research Council (BBSRC) (T.P.J.K.), the Gates Cambridge (R.L.) and St. John's Benefactors' Scholarships (J.B.K., R.L.), the Frances and Augustus Newman Foundation (T.P.J.K.) and the EPSRC (K.L.S.). We thank Dr. Francesco Simone Ruggeri for valuable advice and suggestions.

Appendix A. Supplementary data

Supplementary data associated with this article can be found, in the online version, at https://doi.org/10.1016/j.jneumeth.2018.02.005.

References

Alavez, S., Vantipalli, M.C., Zucker, D.J.S., Klang, I.M., Lithgow, G.J., 2012. Amyloid-binding compounds maintain protein homeostasis during ageing and extend lifespan. Nature 472, 226–229.

Aprile, F.A., Sormanni, P., Perni, M., Arosio, P., Linse, S., Knowles, T.P.J., Dobson, C.M., Vendruscolo, M., 2017. Selective targeting of primary and secondary nucleation pathways in Aβ42 aggregation using a rational antibody scanning method. Sci. Adv. 3, e1700488.

Brenner, S., 1974. The genetics of Caenorhabditis elegans. Genetics 77, 71–94.

Buckingham, S.D., Sattelle, D.B., 2009. Fast, automated measurement of nematode swimming (thrashing) without morphometry. BMC Neurosci. 10, 84.

Chalasani, S.H., Chronis, N., Tsunozaki, M., Gray, J.M., Ramot, D., Goodman, M.B., Bargmann, C.I., 2007. Dissecting a circuit for olfactory behaviour in Caenorhabditis elegans. Nature 450, 63–70.

Chiti, F., Dobson, C.M., 2006. Protein misfolding, functional amyloid, and human disease. Annu. Rev. Biochem. 75, 333–366.

Chiti, F., Dobson, C.M., 2017. Protein misfolding, amyloid formation, and human disease: A summary of progress over the last decade. Annu. Rev. Biochem. 86, 27–68.

Cramer, P.E., Cirrito, J.R., Wesson, D.W., Lee, C.Y.D., Karlo, J.C., Zinn, A.E., Casali, B.T., Restivo, J.L., Goebel, W.D., James, M.J., et al., 2012. ApoE-directed therapeutics rapidly clear β-amyloid and reverse deficits in AD mouse models. Science 335, 1503–1506.

Dillin, A., Hsu, A.-L., Arantes-Oliveira, N., Lehrer-Graiwer, J., Hsin, H., Fraser, A.G., Kamath, R.S., Ahringer, J., Kenyon, C., 2002. Rates of behavior and aging specified by mitochondrial function during development. Science 298, 2398–2401.

Faumont, S., Rondeau, G., Thiele, T.R., Lawton, K.J., McCormick, K.E., Sottile, M., Griesbeck, O., Heckscher, E.S., Roberts, W.M., Doe, C.Q., et al., 2011. An image-free opto-mechanical system for creating virtual environments and imaging neuronal activity in freely moving Caenorhabditis elegans. PLoS One 6, e24666.

Fay, D.S., Fluet, A., Johnson, C.J., Link, C.D., 1998. In vivo aggregation of β-amyloid peptide variants. J. Neurochem. 71, 1616–1625.

Feng, Z., Cronin, C.J., Wittig, J.H., Sternberg, P.W., Schafer, W.R., 2004. An imaging system for standardized quantitative analysis of C. elegans behavior. BMC Bioinf. 5, 115.

Gidalevitz, T., Krupinski, T., Garcia, S., Morimoto, R.I., 2009. Destabilizing protein polymorphisms in the genetic background direct phenotypic expression of mutant SOD1 toxicity. PLoS Genet. 5, e1000399.

Habchi, J., Arosio, P., Perni, M., Costa, A.R., Yagi-Utsumi, M., Joshi, P., Chia, S., Cohen, S.I.A., Muller, M.B.D., Linse, S., et al., 2016. An anticancer drug suppresses the primary nucleation reaction that initiates the production of the toxic Ab 42 aggregates linked with Alzheimers disease. Sci. Adv. 2, e1501244–e1501244.

Habchi, J., Chia, S., Limbocker, R., Mannini, B., Ahn, M., Perni, M., Hansson, O., Arosio, P., Kumita, J.R., Challa, P.K., et al., 2017. Systematic development of small molecules to inhibit specific microscopic steps of Aβ42 aggregation in Alzheimer's disease. Proc. Natl. Acad. Sci. U. S. A. 114, E200–E208.

Hahm, J.-H., Kim, S., DiLoreto, R., Shi, C., Lee, S.-J.V., Murphy, C.T., Nam, H.G., 2015. C. elegans maximum velocity correlates with healthspan and is maintained in worms with an insulin receptor mutation. Nat. Commun. 6, 8919.

Hamilton, B., Dong, Y., Shindo, M., Liu, W., Odell, I., Ruvkun, G., Lee, S.S., 2005. A systematic RNAi screen for longevity genes in C elegans. Genes Dev. 19, 1544–1555.

Hardaker, L.A., Singer, E., Kerr, R., Zhou, G.T., Schafer, W.R., 2001. Serotonin modulates locomotory behavior and coordinates egg-laying and movement in Caenorhabditis elegans. J. Neurobiol. 49, 303–313.

Hsin, H., Kenyon, C., 1999. Signals from the reproductive system regulate the lifespan of C-elegans. Nature 399, 362–366.

Husson, S.J., Costa, W.S., Schmitt, C., Gottschalk, A., 2012. Keeping track of worm trackers. In: WormBook., pp. 1–17.

Jorgensen, E.M., Mango, S.E., 2002. The art and design of genetic screens: caenorhabditis elegans. Nat. Rev. Genet. 3, 356–369.

Kenyon, C.J., 2010. The genetics of ageing. Nature 464, 504–512.

Kim, Y., Sun, H., 2007. Functional genomic approach to identify novel genes involved in the regulation of oxidative stress resistance and animal lifespan. Aging Cell 6, 489–503.

Klass, M.R., 1983. A method for the isolation of longevity mutants in the nematode caenorhabditis-elegans and initial results. Mech. Ageing Dev. 22, 279–286.

Knowles, T.P.J., Vendruscolo, M., Dobson, C.M., 2014. The amyloid state and its association with protein misfolding diseases. Nat. Rev. Mol. Cell Biol. 15, 384–396.

Lee, S.S., Kennedy, S., Tolonen, A.C., Ruvkun, G., 2003. DAF-16 target genes that control C. elegans life-span and metabolism. Science 300, 644–647.

Leifer, A.M., Fang-Yen, C., Gershow, M., Alkema, M.J., Samuel, A.D.T., 2011. Optogenetic manipulation of neural activity in freely moving Caenorhabditis elegans. Nat. Methods 8, 147–152.

Link, C.D., 1995. Expression of human beta-amyloid peptide in transgenic Caenorhabditis elegans. Proc. Natl. Acad. Sci. U. S. A. 92, 9368–9372.

Lublin, A.L., Link, C.D., 2013. Alzheime's disease drug discovery: in vivo screening using Caenorhabditis elegans as a model for β-amyloid peptide-induced toxicity. Drug Discov. Today Technol. 10, e115–e119.

Machino, K., Link, C.D., Wang, S., Murakami, H., Murakami, S., 2014. A semi-automated motion-tracking analysis of locomotion speed in the C. elegans transgenics overexpressing beta-amyloid in neurons. Front. Genet. 5, 202.

McColl, G., Roberts, B.R., Pukala, T.L., Kenche, V.B., Roberts, C.M., Link, C.D., Ryan, T.M., Masters, C.L., Barnham, K.J., Bush, A.I., et al., 2012. Utility of an improved model of amyloid-beta ($A\beta_{1-42}$) toxicity in Caenorhabditis elegans for drug screening for Alzheimer's disease. Mol. Neurodegener. 7, 57.

Morley, J.F., Brignull, H.R., Weyers, J.J., Morimoto, R.I., 2002. The threshold for polyglutamine-expansion protein aggregation and cellular toxicity is dynamic and influenced by aging in Caenorhabditis elegans. Proc. Natl. Acad. Sci. U. S. A. 99, 10417–10422.

Nahabedian, J.F., Qadota, H., Stirman, J.N., Lu, H., Benian, G.M., 2012. Bending amplitude? A new quantitative assay of C identification of phenotypes for mutants in genes encoding muscle focal adhesion components elegans locomotion. Methods 56, 95–102.

Nollen, E.A.A., Garcia, S.M., van Haaften, G., Kim, S., Chavez, A., Morimoto, R.I., Plasterk, R.H.A., 2004. Genome-wide RNA interference screen identifies previously undescribed regulators of polyglutamine aggregation. Proc. Natl. Acad. Sci. U. S. A. 101, 6403–6408.

Nussbaum-Krammer, C.I., Neto, M.F., Brielmann, R.M., Pedersen, J.S., Morimoto, R.I., 2015. Investigating the spreading and toxicity of prion-like proteins using the metazoan model organism C. elegans. J. Vis. Exp., p52321.

Perni, M., Galvagnion, C., Maltsev, A., Meisl, G., Muller, B.D., Challa, P.K., Kirkegaard, J.B., Flagmeier, P., Cohen, S.I.A., et al., 2017a. A natural product inhibits the initiation of a-synuclein aggregation and suppresses its toxicity. Proc. Natl. Acad. Sci. U. S. A. 114, E1009–E1017.

Perni, M., Aprile, F.A., Casford, S., Mannini, B., Sormanni, P., Dobson, C.M., Vendruscolo, M., 2017b. Delivery of native proteins into C. elegans using a transduction protocol based on lipid vesicles. Sci. Rep. 7, 7380.

Petrascheck, M., Miller, D.L., 2017. Computational analysis of lifespan experiment reproducibility. Front. Genet. 8, 92.

Ramot, D., Johnson, B.E., Berry, T.L., Carnell, L., Goodman, M.B., 2008. The Parallel Worm Tracker: a platform for measuring average speed and drug-induced paralysis in nematodes. PLoS One 3, e2208.

Restif, C., Ibáñez-Ventoso, C., Vora, M.M., Guo, S., Metaxas, D., Driscoll, M., 2014. CeleST: computer vision software for quantitative analysis of C. elegans swim behavior reveals novel features of locomotion. PLoS Comput. Biol. 10, e1003702.

Sarin, S., Prabhu, S., O'Meara, M.M., Pe'er, I., Hobert, O., 2008. Caenorhabditis elegans mutant allele identification by whole-genome sequencing. Nat. Methods 5, 865–867.

Solis, G.M., Petrascheck, M., 2011. Measuring Caenorhabditis elegans Life Span in 96 Well Microtiter Plates. J. Vis. Exp. 49, 2496.

Soto, C., 2003. Unfolding the role of protein misfolding in neurodegenerative diseases. Nat. Rev. Neurosci. 4, 49–60.

Stirman, J.N., Crane, M.M., Husson, S.J., Wabnig, S., Schultheis, C., Gottschalk, A., Lu, H., 2011. Real-time multimodal optical control of neurons and muscles in freely behaving Caenorhabditis elegans. Nat. Methods 8, 153–158.

Stroustrup, N., Ulmschneider, B.E., Nash, Z.M., López-Moyado, I.F., Apfeld, J., Fontana, W., 2013. The caenorhabditis elegans lifespan machine. Nat. Methods 10, 665–670.

Swierczek, N.A., Giles, A.C., Rankin, C.H., Kerr, R.A., 2011. High-throughput behavioral analysis in C. elegans. Nat. Methods 8, 592–598.

Tsechpenakis, G., Bianchi, L., Metaxas, D., Driscoll, M., 2008. A novel computational approach for simultaneous tracking and feature extraction of C. elegans populations in fluid environments. IEEE Trans. Biomed. Eng. 55, 1539–1549.
Tsibidis, G.D., Tavernarakis, N., 2007. Nemo: a computational tool for analyzing nematode locomotion. BMC Neurosci. 8, 86.
Van Ham, T.J., Thijssen, K.L., Breitling, R., Hofstra, R.M.W., Plasterk, R.H.A., Nollen, E.A.A., 2008. C. elegans model identifies genetic modifiers of α-synuclein inclusion formation during aging. PLoS Genet. 4, e1000027–11.
Van Ham, T.J., Holmberg, M.A., Van der Goot, A.T., Teuling, E., Garcia-Arencibia, M., Kim, H.-E., Du, D., Thijssen, K.L., Wiersma, M., Burggraaff, R., et al., 2010. Identification of MOAG-4/SERF as a regulator of age-related proteotoxicity. Cell 142, 601–612.
Van der Goot, A.T., Nollen, E.A.A., 2013. Tryptophan metabolism: entering the field of aging and age-related pathologies. Trends Mol. Med. 19, 336–344.
Van der Goot, A.T., Zhu, W., Vazquez-Manrique, R.P., Seinstra, R.I., Dettmer, K., Michels, H., Farina, F., Krijnen, J., Melki, R., Buijsman, R.C., et al., 2012. Delaying aging and the aging-associated decline in protein homeostasis by inhibition of tryptophan degradation. Proc. Natl. Acad. Sci. U. S. A. 109, 14912–14917.
Wang, S.J., Wang, Z.-W., 2013. Track-a-worm, an open-source system for quantitative assessment of C. elegans locomotory and bending behavior. PLoS One 8, e69653.
Wood, H., 2016. Alzheimer disease: anticancer drug prevents nucleation of toxic amyloid-β42 aggregates. Nat. Rev. Neurosci. 12, 126.
Wu, Y., Wu, Z., Butko, P., Christen, Y., Lambert, M.P., Klein, W.L., Link, C.D., Luo, Y., 2006. Amyloid- −induced pathological behaviors are suppressed by ginkgo biloba extract EGb 761 and ginkgolides in transgenic caenorhabditis elegans. J. Neurosci. 26, 13102–13113.
Yemini, E., Jucikas, T., Grundy, L.J., Brown, A.E.X., Schafer, W.R., 2013. A database of Caenorhabditis elegans behavioral phenotypes. Nat. Methods 10, 877–879.